# Crystallization of Canasite/Frankamenite-Based Glass-Ceramics

Cheryl A. Miller,*,† Ian M. Reaney, Paul V. Hatton, and Peter F. James

*Sir Robert Hadfield Building, The University of Sheffield, Mappin Street, Sheffield, S1 3JD, U.K.*

*Received June 30, 2004. Revised Manuscript Received September 23, 2004*

Glass-ceramics based on the naturally occurring quadruple chain silicate, canasite ($Na_4K_2Ca_5Si_{12}O_{30}F_4$), have been produced. The phase evolution of these materials has been investigated using differential thermal analysis (DTA), X-ray diffraction (XRD), and scanning and transmission electron microscopy (SEM and TEM). Two sequences of nucleation and growth have been identified. When $CaF_2$ crystals are present prior to the formation of the chain silicate phases, canasite and frankamenite (a fluorine-rich form of canasite) are the major crystalline phases at (>750 °C) along with minor phases of xonotlite and cristobalite depending on temperature. If $CaF_2$ forms, frankamenite is the major crystalline phase between 750 and 850 °C but is replaced by xonotlite at >850 °C. It is postulated therefore that the presence of $CaF_2$ crystals is a prerequisite for the formation of true canasite glass-ceramics.

## 1. Introduction

The canasite mineral was discovered in Khibin, Russia, and was described by Dorfman et al. in 1959,[3] with a subsequent paper in 1960.[4] Chiragov et al.[5] confirmed the original X-ray data of Dorfman et al.[3,4] and defined the chemical formula as $Ca_5Na_4K_2[Si_{12}O_{30}](OH,F)_4$. The crystal structure was described as being based on four wollastonite chains, linked together to form a tubular unit running along the *b*-axis. These tubes are connected to edge-shared $Na(O,F)_6$ (primarily) and $Ca(O,F)_6$ octahedra.[1,2] Rozhdestvenskaya et al.[6] reported that the Si−O−Si angles in the chains are very similar to those in pectolite.

The four wollastonite chains can also be viewed as two xonotlite chains. Xonotlite $Ca_6[Si_6O_{17}](OH)_2$ is a rare mineral formed in hyper-alkaline, hydrothermal environments.[7] The crystals of xonotlite are needlelike in morphology and have a high aspect ratio.[8] It is a double chain silicate in which the chains (comparable to those in wollastonite) run parallel to the *b*-axis.[7,9] It is monoclinic with a *P*2/*a* space group.

More recently, Nikishova et al.[10] reported a fluorine analogue of canasite found in Yakutia which they analyzed using X-ray and electron diffraction. They concluded that canasite in Yakutia was structurally different from that found in Khibin. In 1996, the Commission on New Minerals and Mineral Names of the International Mineralogical Association changed the nomenclature of the Yukutian canasite to frankamenite,[11] despite this compound being reported as canasite-A in the JCPDS database. The main difference is that frankamenite is triclinic, has excess free water, and F is dominant over OH as compared to monoclinic canasite. This leads to changes in the ordering of Ca and Na cations within the structure.[11] X-ray powder patterns of canasite and frankamenite are similar, except that there are 12 weak reflections in the high $2\theta$ region for frankamenite absent in canasite.

Although several groups have studied glass-ceramics based on canasite, to date, none of the work published on synthesized canasites, including Beall,[1,2,12−14] Oguma et al.,[15] Likitvanichkul and Lacourse,[16] Anusavice and Zhang,[17,18] Zhang and Anusavice,[19] and Johnson et al.,[20,21] discusses frankamenite or canasite-A (CA). The

* Corresponding author. Fax: +44 115 951 3764. E-mail: cheryl.miller@nottingham.ac.uk.

† Current address: School of Mechanical, Materials, and Manufacturing Engineering, Wolfson Building, University of Nottingham, Nottingham NG7 2RD, U.K.

(1) Beall, G. H. U.S. patent 4,386,162, 1983.
(2) Beall, G. H. U.S. patent 4,397,670, 1983.
(3) Dorfman, M. D. *Am. Mineral.* **1959**, *44*, 909.
(4) Dorfman, M. D.; Rogachev, D. D.; Goroshchenko, Z. I.; Uspenskaya, E. I. *Am. Mineral.* **1960**, *45*, 253.
(5) Chiragov, M. I.; Mamedov, Kh. S.; Belov, N. V. *Dokl. Acad. Nauk USSR* **1969**, *185*, 96.
(6) Rozhdestvenskaya, I. V.; Nikishova, L. V.; Bannova, I. I.; Lazebnik, Y. D. *Mineral. Zh.* **1988**, *10*, 31.
(7) Shaw, S.; Clark, S. M.; Henderson, C. M. B. *Chem. Geol*. **2000**, *167*, 129.
(8) Bellmann, B.; Muhle, H. *Environ. Health Perspect.* **1994**, *102*, 191.
(9) Mamedov, K. S.; Belov, N. V. *Dokl. Akad. Nauk SSSR* **1955**, *104*, 615.
(10) Nikishova, L. V.; Lazebnik, K. A.; Rozhdestvenskaya, I. V.; Dazebnik, Y. D.; Yemelayanova, N. N. *Mineral. Zh.* **1992**, *14*, 71.
(11) Rozhdestvenskaya, I. V.; Nikishova, L. V.; Lazebnik, Y. D. *Mineral. Mag.* **1996**, *60*, 897.
(12) Beall, G. H.; Chyung, K.; Stewart, R. L.; Donaldson, K. Y.; Lee, H. L.; Baskaran, S.; Hasselman, D. P. H. *J. Mater. Sci.* **1986**, *21*, 2365.
(13) Beall, G. H. *J. Non-Cryst. Solids* **1991**, *129*, 163.
(14) Beall, G. H. *Annu. Rev. Mater. Sci.* **1992**, *22*, 91.
(15) Oguma, M.; Chyung, K.; Donaldson, K. Y.; Hasselman, D. P. H. *J. Am. Ceram. Soc.* **1987**, *70*, C-2−C-3.
(16) Likitvanichkul, S.; Lacourse, W. C. *J. Mater. Sci.* **1995**, *30*, 6151.
(17) Anusavice, K. J.; Zhang, N. Z. *J. Dent. Res.* **1998**, *77*, 1553.
(18) Anusavice, K. J.; Zhang, N. Z. *J. Dent. Res.* **1998**, *75*, 67.
(19) Zhang, N. Z.; Anusavice, K. J. *J. Am. Ceram. Soc.* **1999**, *82*, 2509.
(20) Johnson, A.; Shareef, M. Y.; Walsh, J. M.; Hatton, P. V.; van Noort, R.; Hill, R. G. *Dent. Mater.* **1998**, *14*, 412.

10.1021/cm048946l CCC: $27.50 
Published on Web 12/01/2004

**Table 1. Glass Batch Compositions (mol %)**

| | $SiO_2$ | CaO | $Na_2O$ | $K_2O$ | $CaF_2$ | $Al_2O_3$ |
|---|---|---|---|---|---|---|
| CANA 1 | 62.00 | 12.80 | 9.50 | 5.60 | 8.80 | 1.30 |
| CANA 2 | 60.00 | 15.00 | 10.00 | 5.00 | 10.00 | 0.00 |
| CANA 3 | 63.46 | 15.87 | 4.80 | 5.29 | 10.58 | 0.00 |
| CANA 4 | 61.62 | 19.18 | 3.80 | 5.13 | 10.27 | 0.00 |

exception is Miller et al.,[22,23] who found that the XRD traces obtained from materials based on compositions developed by Beall[1,2] crystallize to a mixture of canasite and canasite-A (frankamenite). As a consequence of this confusion, the properties (e.g., fracture toughness, durability, and bend strength) of the respective phases have become obscured. Rozhdestvenskaya et al.[11] have commented that water molecules contained in the frankamenite silicate chains act to reduce the intensity of the ion charge, resulting in weakening of the structure. Moreover, in frankamenite, $F^-$ is dominant over $OH^-$, which according to Rozhdestvenskaya et al.[11] further weakens the crystal lattice. On the other hand, the $OH^-$ groups in canasite stabilize the structure via hydrogen bonding between the octahedra and silica chains.

In a recent article, Miller et al.[23] identified several canasite compositions modified from the stoichiometric formula, $Na_4K_2Ca_5Si_{12}O_{30}F_4$,[1,2] by adding either $P_2O_5$ or altering the molar ratios of $Na_2O$ and CaO. The modified compositions were bioactive in simulated body fluid, whereas a Corning reference material optimized principally for strength and containing $Al_2O_3$ was bioinert. The phase evolution in $P_2O_5$-doped canasite compositions will be dealt with in a separate article. Here, the phase evolution of the $Na_2O$ and CaO modified compositions is investigated.

## 2. Experimental Procedure

**2.1. Preparation of Glass-Ceramics.** Standard laboratory reagent (SLR, Fisher scientific) grade $CaCO_3$ (CaO), $Na_2CO_3$ ($Na_2O$), $K_2CO_3$ ($K_2O$), and $CaF_2$ along with Loch Aline sand (99.8% $SiO_2$) were used to produce the glass batches listed in Table 1, the exception being CANA 1 which was provided by Corning Inc., USA. Compositions were melted for 2.5−3 h at 1350−1450 °C using an electric furnace in a Pt 2% Rh crucible and were stirred to encourage homogeneity. The use of uncovered crucibles or long melting times leads to volatilization of fluorine as $SiF_4$ and NaF during melting.[16] For this reason, glass melting times were kept as short as possible. The glasses were poured onto warmed steel plates either in boule or in disk form. If there was a likelihood of crystallization, a small amount of the glass was also quenched between two metal plates. To relieve internal stresses, as-cast glasses were annealed in a muffle furnace for 1 h at 420−480 °C, and then cooled at 1 °C $min^{-1}$ to room temperature.

**2.2. Characterization.** Differential thermal analysis (DTA) was used to determine the glass transition ($T_g$) and crystallization temperatures ($T_c$). A Perkin-Elmer DTA 7 with a high-temperature platinum wound furnace was used to heat 10 mg of crushed as-cast glass (~10 $\mu$m) in an Ar atmosphere at a 10 °C $min^{-1}$ heating rate. The same weight of calcined $Al_2O_3$ was used as a reference.

Powder X-ray diffraction (XRD) was used to identify crystalline phases in the materials before and after heat treatment. Powder samples were prepared from bulk material by crushing in a percussion mortar. A Philips diffractometer (Eindhoven, Holland) was used with Cu Kα radiation, and spectra were obtained from 10° to 70° 2$\theta$, at a step size of 0.02° and at a scanning speed of 2° $min^{-1}$. Data were analyzed using STOE WinXPOW search and match software (version 2.0, STOE & Cie GmbH, Hilpertstrasse 10, D 64295, Darmstadt).

Thin sections for transmission optical microscopy were prepared by cutting a slice (cross section of ~1 $cm^2$) from the bulk material. One side was ground flat using a coarse diamond impregnated grinding wheel. Further grinding was carried out with silicon carbide paper from 120, down to 1200 grade. The samples were polished on a rotating wheel using 6 $\mu$m followed by 1 $\mu$m diamond paste. The samples were mounted on glass slides (polished side down) with thermoplastic wax (AGr Scientific) and ground to a thickness of 30 $\mu$m. A cover slip was placed over the ground surface using Canada Balsam (Fisher Scientific) as an adhesive. The thin sections were examined under cross-polar conditions using a Polyvar transmitted light microscope.

Fractured and chemically etched samples were examined using scanning electron microscopy (SEM). Fracture surfaces were mounted on an Al Stub using silver dag and gold coated using an Emscope sputtering unit. Etched samples were prepared by grinding and polishing small blocks (1 $cm^3$) to a 1 $\mu$m finish, followed by etching in 10 vol % HF for 15 s. Samples were subsequently mounted on Al stubs with silver dag and gold coated. Samples were examined using either a Camscan series II or a JEOL 6400 SEM operating at 20 kV and at working distances of 25 and 15 mm, respectively. Both microscopes were equipped with LINK energy-dispersive X-ray detectors and ancillary electronics and software used to perform qualitative chemical analysis.

Samples for transmission electron microscopy (TEM) were prepared by mounting thin slices (1 mm × 1 $cm^2$) on a glass slide using a heat-sensitive resin and grinding on both sides to <30 $\mu$m. A 3 mm Cu ring of internal diameter 1000 $\mu$m was then glued onto the sample using epoxy resin. The samples were removed from the slide, and excess material around the edge of the Cu ring was chipped away using a scalpel. Ion beam milling was carried on a Gatan dual mill (Pleasanton, USA) operating at 6 kV with a total beam current of 0.6 $\mu$A and at a 15° angle of incidence. Samples were thinned until perforation and then carbon coated using an Edward's Speedivac (Crawley, UK) evaporation unit. Philips EM 400 and 420 (Einhoven, Holland) and JEOL JEM3010 UHR (Tokyo, Japan) transmission electron microscopes operating at accelerating voltages of 100, 120, and 300 kV, respectively, were used to analyze the samples. All microscopes were equipped with Link energy-dispersive X-ray detectors (EDS) and Oxford Instruments hardware and software to obtain qualitative chemical analyses. Electron diffraction patterns were indexed by comparing experimental patterns to those simulated using Carine (version 3.1) software.

## 3. Results and Discussion

Table 1 lists the as-batched composition of the materials investigated. All compositions formed a clear glass on pouring. Figure 1 shows the DTA traces obtained from as-cast glass powder. The glass transition temperatures ($T_g$) and crystallization temperatures ($T_c$) are indicated, Table 2.

The $T_g$ for CANA 1 was 517 °C, about 30 °C higher than that for the stoichiometric composition (CANA 2, $T_g \approx 490$ °C). However, CANA 1 contains $Al_2O_3$, a highly refractory oxide, which immobilizes alkali ions and hence increases durability. Its presence in a glass is often associated with an increase in $T_g$.[24] Moreover,

(21) Johnson, A.; Shareef, M. Y.; van Noort, R.; Walsh, J. M. *Dent. Mater.* **2000**, *16*, 280.

(22) Miller, C. A.; Reaney, I. M.; Hatton, P. V.; James, P. F. *Glastech. Ber.: Glass Sci. Technol.* **2000**, *73*, 154.

(23) Miller, C. A.; Kokubo, T.; Reaney, I. M.; Hatton, P. V.; James, P. F. *J. Biomed. Mater. Res.* **2002**, *59*, 473.

(24) Paul, A. *Chemistry of Glasses;* Chapman and Hall: London, 1990.

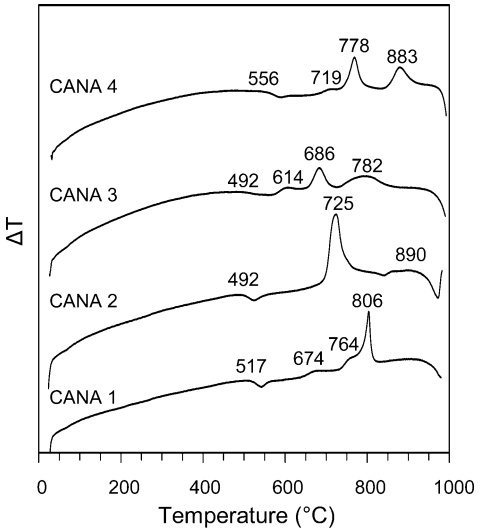


**Figure 1.** DTA traces obtained from "as-cast" glass samples.

**Table 2. Glass Transition and Crystallization Temperatures**

| | $T_g$ (°C) | crystallization peaks (°C) | | |
|---|---|---|---|---|
| CANA 1 | 517 | 674 (B)[a] | 764 (B) | 806 |
| CANA 2 | 492 | 725 | 890 (B) | |
| CANA 3 | 492 | 614 | 686 | 782 |
| CANA 4 | 556 | 719 | 778 | 883 |

[a] (B) indicates a broad peak.

CANA 1 contains less network modifying ions as compared to CANA 2. The $T_g$ for CANA 3 was the same as that for the stoichiometric composition (492 °C). CANA 4 had 1 mol % less $Na_2O$ than CANA 3 in addition to having significantly more CaO than the other compositions. The higher $T_g$ of 556 °C may be attributed to the reduction in monovalent ions and in turn a reduction in nonbridging oxygens. Also, the adverse effect of alkalis on the durability of glass can be counteracted by the addition of divalent network modifiers, especially CaO, which enhances chemical durability. The optimum amount of CaO is thought to be about 10 mol %.[24] However, it has been shown that high lime glasses containing 20 mol % CaO can have good durability provided the soda content is low (5 mol %).[25]

Beall[1,2] proposed that the formation of canasite occurs initially through the crystallization of $CaF_2$ crystals at temperatures in the range of 550−650 °C, which act as heterogeneous nucleating sites for canasite laths (650−950 °C). The validity of this hypothesis is investigated for the compositions shown in Table 1.

The XRD patterns obtained from the isothermal holds for CANA 1 are shown in Figure 2. At temperatures between 550 and 650 °C, the samples become translucent due to the nucleation of $CaF_2$ crystallites. This probably corresponds to the peak at 674 °C in the corresponding DTA trace in Figure 1. Figure 3 is a TEM micrograph showing several $CaF_2$ (0.2 $\mu$m) crystals in CANA 1 heat-treated at 650 °C. The insets are ⟨111⟩ and ⟨110⟩ electron diffraction patterns obtained from the precipitates, confirming the presence of fluorite. By 700 °C, CANA 1 became opaque due to an increase in the degree of crystallinity. Although CANA 1 was provided by Corning Inc., the XRD patterns of the crystalline material did not exactly match the JCPDS data file for canasite [13-0553]. Rather, a mix of canasite and frankamenite (canasite-A) [45-1398] was present, possibly with a minor phase of low-temperature quartz [JCPDS 11-252]. Beall[1,2] also suggested that the peaks did not match perfectly with canasite, stating that "the traces were very similar to those of the naturally occurring minerals" but was unaware of frankamenite which was an unknown mineral in 1983. The phases present in Figure 2 (700 °C) are all silicate-based with similar $d$ spacings. It is proposed therefore that there may be competition between the phases during nucle-

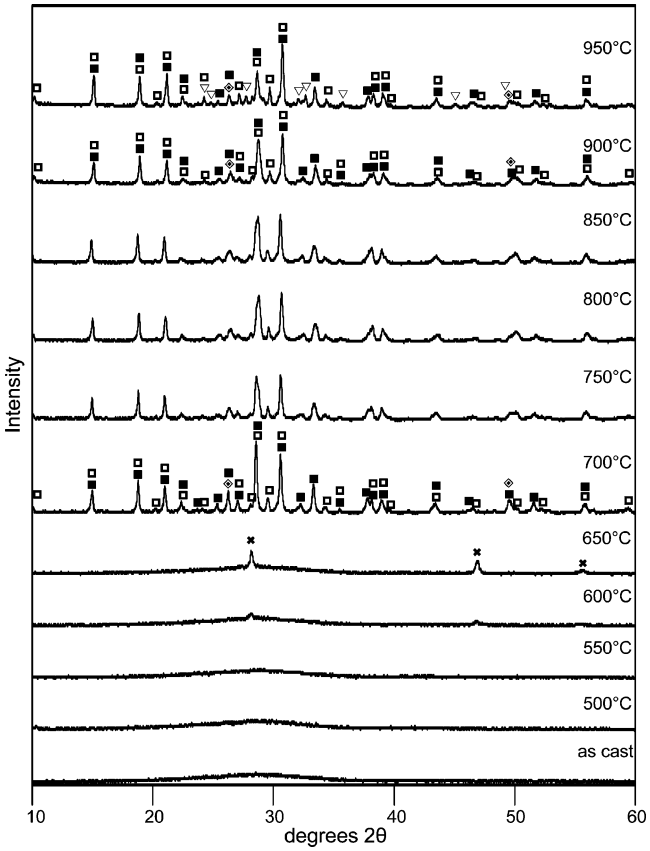


**Figure 2.** XRD series for CANA 1, heat-treated at different isotherms for 2 h, where × represents calcium fluoride, □ represents frankamenite (CA), ■ represents canasite, ◇ represents silica, and ▽ represents xonotlite.

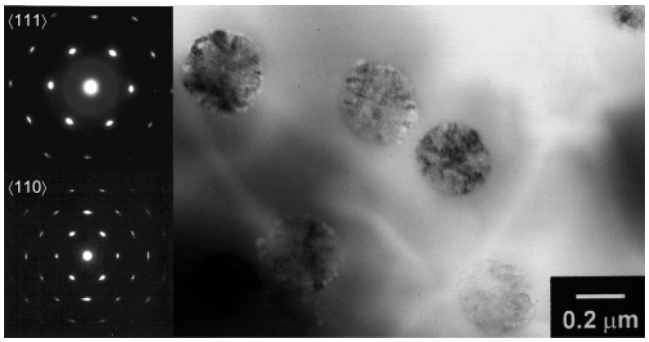


**Figure 3.** Bright field TEM image of CANA 1 heat-treated at 600 °C/2 h showing crystals of $CaF_2$. Inset shows diffraction patterns obtained from the FCC crystals. Arching of the spots suggests that the $CaF_2$ crystals are composed of small crystallites with similar orientations.

(25) Rawson, H. *Inorganic Glass-Forming Systems*; Academic Press: London, 1967.

ation and growth. This may be enhanced by compositional inhomogeneity of the as-cast material, possibly arising from variation in the F concentration due to surface volatilization during melting or by the formation of a F-rich phase ($CaF_2$) prior to nucleation of the chain silicate compound. It should be noted that the naturally occurring mineral phase of canasite, from which the JCPDS data is based, contains $OH^-$ rather than $F^-$ groups. In contrast, the mineral frankemenite contains both $OH^-$ and $F^-$ species with an additional water molecule. However, it is assumed that the chain silicate compounds in the glass-ceramics studied here are principally the fluorinated rather than hydroxy forms of both minerals because ~10 mol % $CaF_2$ is present in the original glass batch.

Because the structures of canasite and frankamenite are similar, certain *d* spacings and therefore angles appear in both mineral XRD spectra, such as those at 27.0°, 28.6°, 30.6°, 38.2°, and 38.9° 2$\theta$. Fortunately, a few peaks are specific to individual phases, 25.3°, 32.2°, 33.3°, 37.8°, and 43.4° 2$\theta$ for canasite and 10.1°, 21.1°, and 29.5° 2$\theta$ for frankamenite. Peaks that correspond to both minerals are labeled with a double symbol; the uppermost symbols represent the most likely phase, as determined by comparing the peak relative intensities and the presence of distinctive peaks. The match for frankamenite (JCPDS 45-1398) is extremely good, with an error of only 0.05° 2$\theta$ (CANA 2 at 750 °C). Nevertheless, peaks that have been assigned solely to canasite and many of the peaks assigned to both canasite and frankamenite have a −0.34° 2$\theta$ error (CANA 1 at 700 °C) with respect to the angles stated for canasite (JCPDS 13-553). This error could be due to the quality of the JCPDS data. Card 13-553 has no quality rating, and there is an uncertainty about the accuracy of the data. In addition, the intensities have been obtained visually and the values have been rounded to the nearest 10. The frankamenite card [45-1398] is rated "I" (indexed), which, although not a star (*) rating, is better than no rating at all.

In a 1983 U.S. patent,[1] Beall stated that the predominant crystalline phases in his formulations were canasite and/or agrellite, $Na_2Ca_4Si_8O_{20}F_2$ and/or fedorite, $(K,Na)_{2.5}(Ca,Na)_7Si_{16}O_{38}(OH,F)_2H_2O$. In addition to canasite and frankamenite, the X-ray patterns in this work have been examined for the presence of these minerals. No evidence was found for agrellite (JCPDS 29-1188), and, although some *d* spacings were coincident with those of fedorite (JCPDS 19-0466), especially at low 2$\theta$ angles, such as those at 14.8°, 19.0°, 20.6°, and 21.1° 2$\theta$, these peaks could also be assigned to frankamenite. In addition, these peaks were found in specimens where the major crystalline phase was undoubtedly frankamenite and the 100% and 90% peaks (30.5 and 49.90° 2$\theta$) of fedorite were absent. Hence, it was concluded that fedorite was not present. Nevertheless, the determination of the exact crystalline phase or phases is extremely difficult, especially when the minerals being investigated have oxide and fluoride components in similar ratios, such as those of canasite, frankamenite (CA), fedorite, xonotlite, and miserite.

In XRD spectra obtained from isothermal holds above 700 °C, the shape of the peaks assigned to canasite also varies in CANA 1 (Figure 2). At 700 °C, the main canasite peak at 28.7° 2$\theta$ is sharp, and there is a double peak at 37.9/38.3° 2$\theta$ (canasite/canasite and frankamenite). However, at temperatures in the range of 750−900 °C, the 100% canasite peak (28.5° 2$\theta$) has broadened and reduced in intensity. Other peaks assigned exclusively to canasite (e.g., 33.3° 2$\theta$) have also weakened, and the canasite shoulder (37.8° 2$\theta$) of the double peak is no longer resolvable (Figure 2). In contrast, the peaks ascribed to frankamenite remain virtually constant with respect to position and intensity throughout the temperature range. There are several possible explanations. First, the change in shape could be due to a change in the molar ratio of ions in the canasite phase, which depends on the exact temperature of heat-treatment. A more plausible reason is that the frankamenite phase becomes more dominant with increasing heat-treatment temperature; that is, at 700 °C the ratio of the peaks at 28.5° and 30.6° 2$\theta$ indicates that canasite is dominant but by 900 °C the ratio is reversed suggesting that frankamenite is now predominant. Hence, the peak at 28.7° 2$\theta$ becomes broader as the frankamenite 19% peak at 28.9° 2$\theta$ becomes more intense and the lower intensity canasite peaks, for example, 32.2°, 33.3°, and 37.9° 2$\theta$ fade.

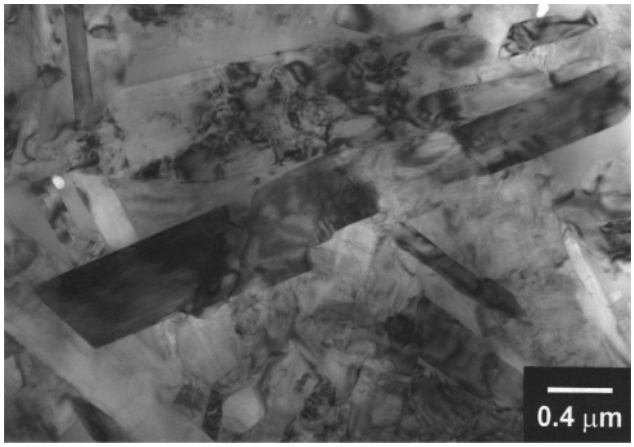


**Figure 4.** Bright field TEM image of CANA 1 heat-treated at 520 °C/2 h followed by 800 °C/2 h showing laths of canasite.

The DTA trace for CANA 1 (Figure 1) showed a broad peak at 674 °C, followed by a shoulder at 764 °C and major peak at 806 °C. It is proposed that the first peak is due to growth of fluorite crystals (674 °C), and the second and third peaks are attributed to the crystallization of canasite (on the fluorite crystallites, as proposed in 1983 by Beall[1] and frankamenite, respectively).

Figure 4 is a bright field (BF) TEM image of CANA 1, which has been heat-treated at 520 °C/2 h and 800 °C/2 h. The microstructure is composed of laths 0.1−0.5 $\mu$m in width and 1−2 $\mu$m in length. In Beall's work,[1,2,13,14] these laths have been uniformly ascribed to the canasite phase. However, the XRD data presented here for samples heat-treated above 700 °C cast doubt on this interpretation. More likely, the laths are a mix of canasite and frankamenite. Electron diffraction patterns from the laths are shown in Figure 5, but these have not been indexed as it was impossible to distinguish directly between the phases as the structures all have large *d* spacings and low symmetry, that is, monoclinic (canasite) and triclinic (frankamenite). Dis-

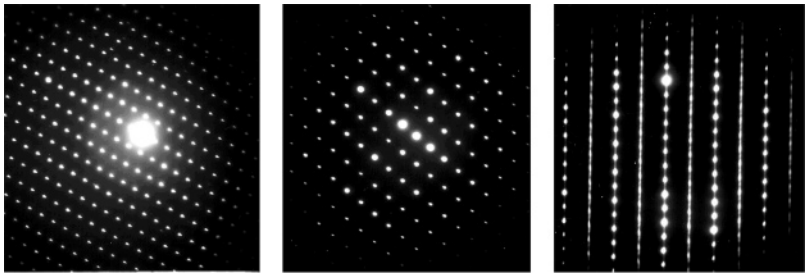

**Figure 5.** Electron diffraction patterns obtained from the lathlike structures in CANA 1 heat-treated at 520 °C/2 h followed by 800 °C/2 h as shown in Figure 4.

tinguishing between zone axes, therefore, becomes an almost impossible task without more accurate ionic positions and lattice parameters for the canasite and frankamenite phases so that simulations may be performed.

On heat-treating at 950 °C, phases other than canasite, frankamenite, and quartz were observed. Additional peaks at 24.8°, 27.7°, 35.7°, and 45.1° 2$\theta$ were detected, the small frankamenite peak at 32.3° 2$\theta$ split in two (32.1° and 32.7° 2$\theta$) and the intensity of the frankamenite peak at 24.3° 2$\theta$ increased. These new peaks matched the $d$ spacing of a calcium silicate phase, xonotlite ($Ca_6Si_6O_{17}(OH)_2$: JCPDS 23-125). In the case of CANA 1 at 950 °C, all of the xonotlite peaks greater than 20% have been accounted for. However, there is some overlap with existing peaks such as those at 29.9° and 46.6° 2$\theta$. Unfortunately, the $d$ spacing of 3.080 Å (28.97° 2$\theta$) equates to the 100% peak for xonotlite and canasite and the 19% peak for frankamenite. This overlapping is inevitable, as the three phases (canasite, frankamenite, and xonotlite) present in CANA 1 at 950 °C are calcium silicates with comparable structures and $d$ spacings, dictated by the chainlike configuration of their tetrahedral building units. The canasite (hence frankamenite) structure has even been described as two xonotlite[5] or pectolite[6] chains joined together. Scott[26] also noted that the chains in miserite are similar to those of pectolite, but this phase was not detected in XRD traces.

The crystallization behavior of even "well-characterized" canasite glass-ceramics developed by Beall is complex with competition between at least three silicate phases as temperature increases. The previous section describes the general trends that occur in the phase evolution as a function of temperature, but some details remain unresolved. For example, the shoulder of the double peak at 38° 2$\theta$ indexed to canasite, which is present at 700 °C, disappears at 800 °C, but reappears at 950 °C, indicating that the solid solution of canasite at 950 °C is similar to that at 700 °C. From analyses of all XRD traces, it seems only the peaks labeled as canasite change in appearance, whereas those associated with frankamenite do not. It is suggested therefore that the composition of frankamenite remains virtually constant with temperature and from glass to glass, whereas the canasite phase varies in composition which may be a result of the inherent solid solution behavior of the canasite phase.[1,2]

Although heat-treatments have been carried out at 50 °C intervals between 500 and 950 °C, for the remaining series only XRD traces from samples heat-treated at temperatures, which show changes in the phase assemblage, are shown and discussed.

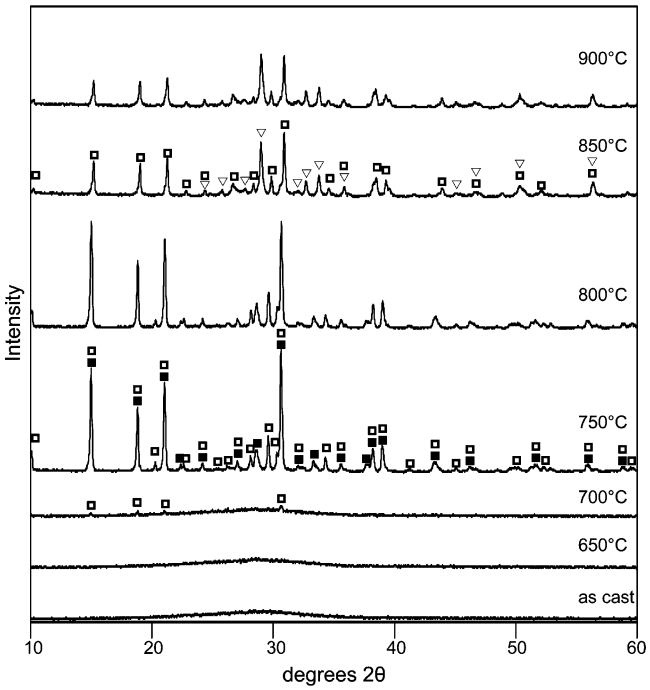


**Figure 6.** XRD series for CANA 2, heat-treated at different isotherms for 2 h, where □ represents frankamenite (CA), ■ represents canasite, and ▽ represents xonotlite.

Glass CANA 2 has the stoichiometric canasite composition, as proposed by Beall.[1] For heat-treatment temperatures up to 650 °C, the glass sample remained clear and XRD traces showed an amorphous structure (Figure 6), confirming that no crystallization had occurred. The major (first) crystallization peak for CANA 2 on the DTA is at 725 °C, and samples heat-treated at 700 °C displayed peaks in the XRD spectra. These peaks increased in intensity when samples were heat-treated at 800 °C and the majority of peaks matched well with those of frankamenite (JCPDS 45-1398), with a very small error of ±0.05° 2$\theta$. Exceptions were found at 28.6°, 33.3°, and 37.8° 2$\theta$. These peaks correspond to canasite (JCPDS 13-0553), and when the error factor of 0.34° 2$\theta$ from section 4.3.1 is added, they compare extremely well with peaks observed in CANA 1. Although some canasite peaks are undoubtedly present, the actual amount is minor as many peaks are absent or weak, including the 100% peak at 29.0° 2$\theta$. Hence, up to and including 800 °C, CANA 2 is mainly composed of frankamenite, which forms without the presence of $CaF_2$ crystals, suggesting the possibility that homogeneous nucleation

(26) Scott, J. D. *Can. Mineral.* **1976**, *14*, 31.

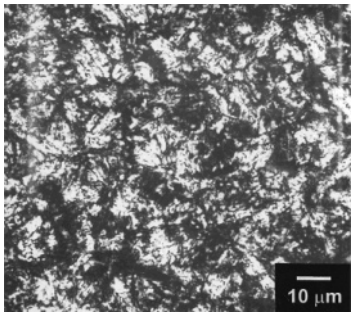


**Figure 7.** Optical micrograph of heat-treated CANA 2 showing frankamenite spherulites.

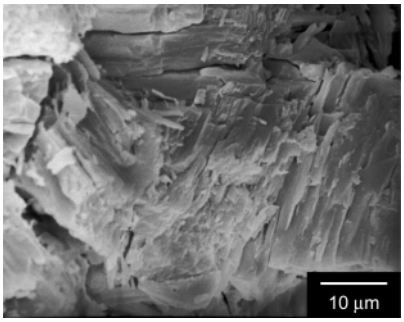


**Figure 8.** SEM micrograph of heat-treated CANA 2 showing frankamenite spherulites.

may have occurred. Moreover, samples heat-treated between 700 and 800 °C sagged. This was probably due to an insufficient density of nuclei/crystallites within the glassy matrix that would normally stiffen the specimen and prevent sagging.

The DTA trace of CANA 2 exhibits a broad peak with its onset at approximately 850 °C, which is coincident with significant changes in the XRD traces obtained from samples heat treated at 800 and 850 °C. As compared to 800 °C, the trace at 850 °C showed a decrease in intensity of all frankamenite peaks; moreover, the samples did not deform during heat-treatment. Initially, it was thought that the intensity of the canasite peaks had increased, but the 100% peak was at 29.0° 2$\theta$, whereas for canasite it is expected at 28.6° 2$\theta$. Another unexplained shift was also apparent; a canasite peak should be present at 33.3° 2$\theta$, whereas in the 850 °C sample it occurred at 33.8° 2$\theta$. At first, it was thought this could be explained by solid solution effects, but other canasite peaks that were present at 750−800 °C (22.4° and 37.8° 2$\theta$) were no longer resolvable. Moreover, new peaks appeared at 27.7°, 32.1°, 32.7°, and 45.1° 2$\theta$. The simplest explanation for the observed diffraction data is the crystallization of a xonotlite phase.

The appearance of xonotlite and the dominance of frankamenite over canasite at higher temperature in CANA 2 is a phase evolution similar to that in described in CANA 1. The difference here is that canasite is always a minor phase, and not present above 850 °C. It has been proposed by Beall[1,2] that canasite nucleates on fluorite crystallites. Therefore, according to Beall,[1,2] it may be concluded that canasite is absent in CANA 2 because $CaF_2$ is absent; that is, canasite will only nucleate heterogeneously from the glass matrix on $CaF_2$, whereas frankamenite appears to nucleate homogeneously. Consequently, at higher temperatures in CANA 2, frankamenite dominates followed by the crystallization of xonotlite.

Transmission optical microscopy obtained from a sample heat-treated at 520 °C/2 h and 800 °C/2 revealed large spherulites (20−30 $\mu$m) of frankamenite in which striations (laths) (10−15 $\mu$m) were observed (Figure 7). Figure 8 shows a SEM micrograph of a fracture surface of the same material. The laths formed in CANA 2 were large as compared to those observed in Corning canasite (CANA 1) (2−3 $\mu$m). The larger laths may have arisen because a low number of nuclei were formed and frankamenite was able to crystallize without competition from other phases.

In CANA 1 (provided by Corning Inc.), both canasite and frankamenite compete during crystallization at ~800 °C. From the above data, it is suggested that canasite is favored in regions where $CaF_2$ crystallites are present and frankamenite homogeneously nucleates in the bulk away form these crystallites. As the two phases grow, the residual glass composition will vary from point to point depending on whether it is adjacent to canasite or frankamenite. In effect, this inhibits further crystal growth because distances for the correct ions to diffuse to the crystal growth front become longer. In CANA 2 at <850 °C, this situation does not occur as frankamenite is the single major crystalline phase. The presence of a dominant crystal phase growing without competition gives rise to a coarse, large grained microstructure and results in poor mechanical properties, as evidenced by the crumbling of CANA 2 during polishing. However, this was not the case for CANA 2 heat-treated at or above 850 °C. At this temperature, there is once again competition between phases during crystal growth, in this case between frankamenite and xonotlite rather than frankamenite and canasite, and samples may be polished and machined without crumbling.

CANA 3 was prepared with 4.8 mol % rather than 10 mol % $Na_2O$. Figure 9 shows the XRD traces for as-cast CANA 3, isothermally heat-treated at different temperatures for 2 h. CANA 3 poured clear and was found to be fully amorphous by XRD in the as-cast state, and, like CANA 1, the first crystalline phase to appear was $CaF_2$ at 550 °C. After heat-treatment at 700 °C, the specimen became translucent. $CaF_2$ peaks were still present, but new peaks had appeared that could be indexed according to a mixed phase assemblage of canasite and frankamenite. Minor peaks of xonotlite were also present.

Heat-treating CANA 3 at 800 °C resulted in an opaque sample. The canasite, frankamenite, and xonotlite peaks increased in intensity, but $CaF_2$ peaks were no longer resolvable. At 900 °C, the relative intensity of the xonotlite peaks decreased, becoming only a minor phase, similar to the Corning material (CANA 1). However, new peaks at 21.9° and 35.7° 2$\theta$ were observed which were indexed according to cristobalite [JCPDS 27-605]. Although these new peaks shifted slightly to 22.1° and 36.2° 2$\theta$ at 950 °C, they could still be indexed as cristobalite [JCPDS 39-1425], which was never observed in CANA 1.

The DTA trace for CANA 3 shows three broad exotherms at ~614, 686, and 782 °C. It is difficult to interpret exactly the crystallization sequence, but from the XRD data, the likely crystallization sequence is the

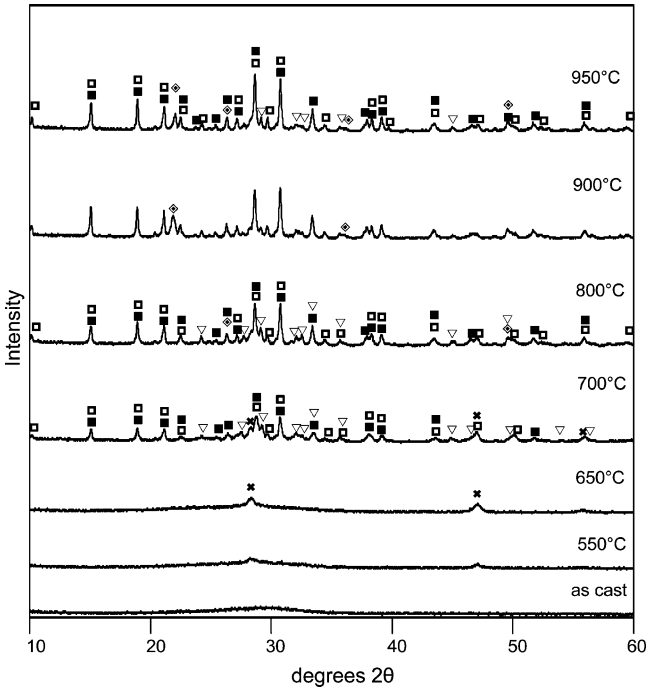


**Figure 9.** XRD series for CANA 3, heat-treated at different isotherms for 2 h, where × represents calcium fluoride, ▽ represents xonotlite, □ represents frankamenite (canasite-A), ■ represents canasite, and ◇ represents a silica phase.

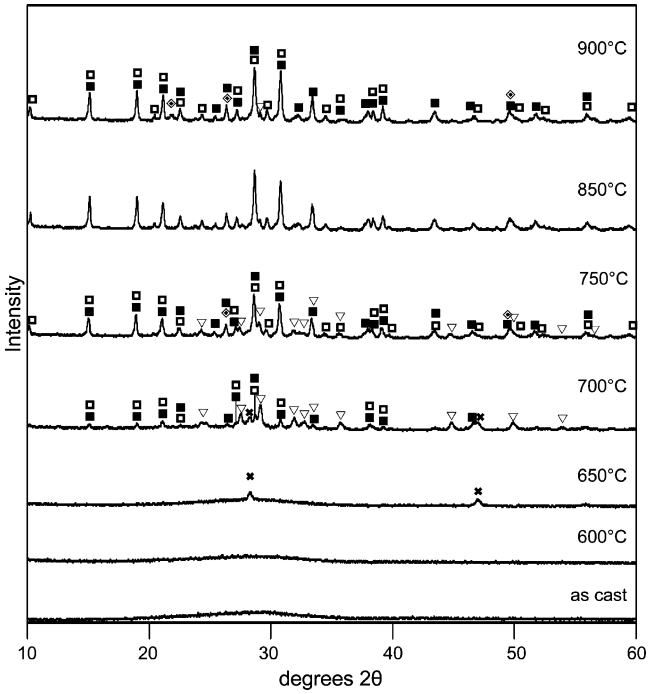


**Figure 10.** XRD series for CANA 4, heat-treated at different isotherms for 2 h, where × represents calcium fluoride, ▽ represents xonotlite, □ represents frankamenite (canasite-A), ■ represents canasite, and ◇ represents a silica phase.

formation of $CaF_2$ between 550 and 650 °C, the nucleation of canasite/frankamenite simultaneously observed at 700 °C in XRD traces, followed by xonotlite, which more than doubles in relative intensity between 700 and 800 °C, although this latter exotherm could be due to cristobalite. The formation of the dominant phases, canasite/frankamenite, at approximately the same temperature is responsible for the strongest most intense exotherm at 686 °C.

In previous compositions, xonotlite was not formed until higher temperatures, that is, 850 and 950 °C for CANA 2 and CANA 1, respectively. The crystallization sequence of CANA 3 is similar to CANA 1, that is, at 800 °C, xonotlite, canasite, and frankamenite were all present. Furthermore, $CaF_2$ crystals formed at low temperatures. On the other hand, CANA 2 crystallized to either frankamenite (with minor canasite peaks) at lower temperatures (e.g., 750 °C) or frankamenite and xonotlite at higher temperatures (e.g., 850 °C).

CANA 4 was fabricated with excess CaO with respect to the stoichiometric starting composition, which was compensated by a decrease in the $Na_2O$ concentration. From the DTA trace obtained, $T_g$ occurred at 556 °C and crystallization exotherms were present at 719, 778, and 883 °C. Figure 10 shows the XRD series for as-cast CANA 4 and samples heat-treated for 2 h at different isotherms.

The composition formed $CaF_2$ crystallites at 650 °C corresponding to a DTA exotherm at ~720 °C. As in CANA 3 at 700 °C, fluorite, canasite/frankamenite, and xonotlite were all present in the XRD traces. The onset of crystallization of these phases is responsible for the most intense broad exotherm at 778 °C in the DTA trace. The relative intensities of the xonotlite peaks were greater in CANA 4 than in CANA 3, but it is difficult to distinguish whether canasite or frankamenite was dominant at this temperature.

Samples heat-treated at 750 and 800 °C were opaque in appearance but sagged, suggesting that there was an insufficient degree of crytallinity to stiffen the glassy matrix. The corresponding XRD traces revealed the presence of canasite and frankamenite. $CaF_2$, however, was absent, but minor peaks consistent with quartz could be observed. Above 900 °C, new peaks could be indexed according to cristobalite (thought to be responsible for DTA peaks >880 °C), similar to CANA 3.

## 4. Summary

From the data presented, phase evolution in these compositions is complex and not fully understood. However, some generalizations can be made. There are basically two sequences of nucleation and growth dependent on whether the formation of $CaF_2$ is the first crystallization event. When $CaF_2$ crystals are present, as in CANA 1, 3, and 4, canasite and frankamenite are always the major crystalline phases in samples heat-treated between 750 and 950 °C. The existence of accompanying minor phases depends on both the heat-treatment temperature and the composition. For example, XRD traces from CANA 1 exhibited weak xonotlite peaks at 950 °C. On the other hand, CANA 3 and CANA 4 formed xonotlite with canasite and frankamenite at 700 °C and contained cristobalite at ≥900 °C.

A different crystallization sequence was demonstrated by CANA 2, which did not nucleate $CaF_2$, and frankamenite was the major crystalline phase (750/800 °C). Only small canasite peaks could be observed in XRD traces at 750 °C. Above 800 °C, canasite was no longer present, but xonotlite appeared. Although canasite may be able to form without the prior nucleation of $CaF_2$, it is unstable at higher temperatures where xonotlite is favored.

Generally, it seems that frankamenite will coexist with either canasite or xonotlite, whereas the latter two phases compete directly. The result is that glass-ceramics contain either frankamenite and xonotlite (CANA 2) or frankamenite and canasite as the major phases (CANA 1, 3, and 4) at heat-treatment temperatures $\geq$700 °C.

Although many discrepancies in the phase evolution of canasite-based glass-ceramics are explained in this study, some issues clearly remain unresolved. The most important of these is whether frankamenite crystallizes homogeneously without a prior nucleating phase. The XRD data suggest this to be the case because it is the first phase to form in CANA 2, but there is always the possibility that frankamenite nucleates on a low volume fraction of nanocrystals whose size and volume fraction are below the detection limit of XRD.

**Acknowledgment.** This work was supported by the Andrew Carnegie Research Scholarship from the Institute of Materials, U.K.

CM048946L